AIMS Mathematics, 11(4): 11296–11321.
DOI: 10.3934/math.2026464
Received: 22 February 2026
Revised: 03 April 2026
Accepted: 13 April 2026
Published: 22 April 2026

https://www.aimspress.com/journal/Math

Research article

Families of weighted distributions with inverse-hazard size bias: theory and applications

Ahmed M. Gemeay[1], **Yuri A. Iriarte**[2,*], **Ohud A. Alqasem**[3], **Fatma Masoud A. Zaghdoun**[4] **and Manahil SidAhmed Mustafa**[5]

[1] Department of Mathematics, Faculty of Science, Tanta University, Tanta 31527, Egypt
[2] Departamento de Estadística y Ciencia de Datos, Facultad de Ciencias Básicas, Universidad de Antofagasta, Antofagasta, Chile
[3] Department of Mathematical Sciences, College of Science, Princess Nourah bint Abdulrahman University, P. O. Box 84428, Riyadh 11671, Saudi Arabia
[4] Department of Mathematics, Faculty of Science, Helwan University, Egypt
[5] Department of Statistics, Faculty of Science, University of Tabuk, Tabuk, Saudi Arabia

* **Correspondence:** Email: yuri.iriarte@uantof.cl.

Abstract: We studied a new class of weighted distributions in which the weighting mechanism introduces a size bias inversely proportional to the hazard rate of the baseline model. This formulation, referred to as the inverse-hazard size-biased distribution family, provided a flexible framework that unifies and extends several well-known two-parameter models. When one-parameter baseline distributions were considered, classical models such as the gamma, generalized Rayleigh, and beta prime distributions arise as particular cases of the proposed class. Furthermore, two new members based on the Maxwell and half-normal baseline distributions were introduced and studied in detail. Analytical properties, including moments and parameter estimation methods, were derived, and simulation studies were conducted to assess the performance of the estimators. The practical applicability of the proposed models was also illustrated through empirical analyses using real data.

Keywords: weighted distributions; inverse-hazard weighting; size-biased models; flexible parametric models; moment properties; parameter estimation
Mathematics Subject Classification: 62E15, 62E20, 62P12

1. Introduction

A principled and well-established framework for constructing flexible probability models is provided by the theory of weighted distributions. Originally introduced by [1] and later formalized

by [2], weighted distributions arise naturally when the probability of observing a realization depends on a nonnegative weight function reflecting unequal sampling mechanisms, selection bias, or relevance criteria inherent to the data-generating process. Such situations frequently occur in applied fields where observations are recorded with probabilities proportional to their magnitude or associated characteristics.

Early applied studies illustrated how such weighting mechanisms emerge naturally from the observation process itself, as in disease screening programs leading to length-biased sampling [3]. Subsequent theoretical and applied developments formalized weighted and size-biased models and explored their structural properties and implications in reliability and survival analysis; see, for example, [4–6]. Further related results are discussed in [7, 8].

Formally, let X be a random variable with probability density function (PDF) $f(x)$. The corresponding weighted random variable X_w is defined through the PDF

$$f_{X_w}(x) = \frac{w(x)f(x)}{\mu_w}, \quad \mu_w = \mathbb{E}[w(X)], \tag{1.1}$$

where $w(\cdot)$ is a nonnegative weight function. This representation provides a general and flexible mechanism to generate new probability distributions from a given baseline model, while maintaining a clear probabilistic interpretation grounded in the original distributional structure.

In the literature on weighted distributions, the simplest and most classical choice of the weight function is given by powers of the observed variable, namely $w(x) = x^k$, with $k > 0$. When $k = 1$, the resulting distribution corresponds to the so-called size-biased (or length-biased) distribution, whereas the case $k = 2$ leads to the area-biased distribution. The size- and area-biased versions of the Weibull distribution provide illustrative examples of these particular cases (see [9, 10]).

Beyond power-based schemes, alternative weight functions have also been explored in the literature. For instance, authors in [11] introduced a weighted exponential distribution based on a cumulative distribution function (CDF)-dependent weight function given by $w(x) = 1 - e^{-\alpha\lambda x}$, for $\alpha, \lambda > 0$. This construction can be interpreted within a hidden truncation framework [12] or, equivalently, as an Azzalini-type model [13].

Other analytical forms for the weight function have also been considered; see, for example, [14–17]. In these studies, the proposed weighted distributions often give rise to asymmetric shapes and bimodal behavior as a consequence of the weighting mechanism.

The discussion above shows that the weight functions available in the literature primarily focus on the magnitude of the observed data through power-based weighting schemes, on standardized polynomial forms designed to enhance distributional flexibility, and on probability-based constructions such as CDF-dependent weights. Building upon these developments, the present paper introduces families of weighted distributions with inverse-hazard size bias, in which the weighting mechanism combines a classical power-type component with an explicit dependence on the hazard rate of the baseline distribution. This hybrid construction embeds both size-related and reliability-driven information into the probabilistic structure of the model, thereby providing a flexible and interpretable framework for modeling positive continuous data.

The remainder of the paper is organized as follows. In Section 2, we introduce the proposed families of weighted distributions, study their main distributional properties, and derive several special cases, including well-known models from the literature and two new cases based on

half-normal and Maxwell baseline distributions. Section 3 focuses on parameter estimation using the method of moments and maximum likelihood, and includes a Monte Carlo simulation study to assess the finite-sample performance of the estimators under unimodal and monotone decreasing density scenarios. In Section 4, real data applications from engineering contexts are presented to illustrate the practical performance of the proposed models. Finally, Section 5 concludes the paper with a summary of the main findings and directions for future research.

For reproducibility purposes, the R codes used throughout the paper are made publicly available at `https://github.com/YuriIriarte/IHSB-Distributions`.

2. Inverse-hazard size-biased distributions

In this section, we introduce the new family of distributions and study their main distributional properties.

2.1. Generating function

Proposition 1. *Let $X \geq 0$ be a nonnegative continuous random variable with baseline PDF $f(x;\theta)$, reliability function (RF) $R(x;\theta) = \Pr_\theta(X > x)$, and hazard rate function (HRF) $h(x;\theta) = f(x;\theta)/R(x;\theta)$, where $\theta \in \Theta$ denotes the parameter (possibly vector-valued) of the baseline distribution. For $\alpha > 0$ and $\mathbb{E}_\theta[X^\alpha] < \infty$, define*

$$g(x;\alpha,\theta) = \frac{\alpha\, x^{\alpha-1}\, R(x;\theta)}{\mathbb{E}_\theta[X^\alpha]}, \qquad x > 0. \tag{2.1}$$

Then $g(x;\alpha,\theta)$ is a PDF on $(0,\infty)$.

Proof. Since $S(x;\theta) \geq 0$ for all $x > 0$, it follows that $g(x;\alpha,\theta) \geq 0$. Using the moment identity $\mathbb{E}_\theta[X^\alpha] = \alpha \int_0^\infty x^{\alpha-1} R(x;\theta)\, dx$ (see Appendix A), we have

$$\int_0^\infty g(x;\alpha,\theta)\, dx = \frac{\alpha}{\mathbb{E}_\theta[X^\alpha]} \int_0^\infty x^{\alpha-1} R(x;\theta)\, dx = 1.$$

Hence, $g(x;\alpha,\theta)$ integrates to 1 and is therefore a PDF. □

Remark 1. *(a) The PDF $g(\cdot)$ can be expressed in the Rao–Patil weighted form ([5, 6]), given in* (1.1)*, where*

$$w(x;\alpha,\theta) = \alpha\, x^{\alpha-1} \frac{R(x;\theta)}{f(x;\theta)} = \frac{\alpha\, x^{\alpha-1}}{h(x;\theta)}.$$

Thus, this family may be interpreted as a weighted distribution in which the weight function induces a size bias proportional to $x^{\alpha-1}$ and inversely proportional to the hazard rate $h(x;\theta)$. Consequently, observations associated with lower instantaneous risk (smaller hazard) receive greater probability weight, producing a reliability-weighted or tail-weighted version of the parent distribution.

(b) It is worth noting that the use of the RF in the proposed weighting scheme distinguishes the inverse-hazard size-biased (IHSB) family from many existing weighted distributions, which are typically constructed using polynomial weight functions or functions of the baseline CDF. This difference provides an alternative structural perspective for modeling.

(c) When $\alpha = 1$, the weight simplifies to $w(x; 1, \theta) = \frac{1}{h(x;\theta)}$, and the transformed density reduces to $g(x; 1, \theta) = \frac{R(x;\theta)}{\mathbb{E}_\theta[X]}$. In this case the model becomes a pure reliability-weighted distribution, favouring tail observations exclusively through the baseline reliability function. This yields a meaningful probabilistic interpretation: The case $\alpha = 1$ corresponds to a hazard-inverse-weighted distribution that emphasizes observations generated under lower instantaneous risk, a structure that does not coincide with the baseline distribution and remains non trivial within the family.

Definition 1. *A nonnegative random variable X is said to follow an IHSB distribution with parameters $\alpha > 0$ and $\theta \in \Theta$, denoted as $X \sim \text{IHSB}(\alpha, \theta)$, if its PDF is given as in* (2.1).

Remark 2. *Throughout the paper, $\mathbb{E}_\theta(X^\alpha)$ denotes the moment of order α under the baseline distribution indexed by θ. All results involving this quantity are understood to hold under the assumption that the corresponding moment exists and is finite.*

2.2. Stochastic representation

Proposition 2. *Let X be a nonnegative random variable with PDF $f(x; \theta)$ and finite moment $\mathbb{E}_\theta[X^\alpha]$, for some $\alpha > 0$. Let X_w denote the α-size-biased version of X, with PDF*

$$f_{X_w}(x; \alpha, \theta) = \frac{x^\alpha f(x; \theta)}{\mathbb{E}_\theta[X^\alpha]}, \quad x > 0.$$

If $U \sim \text{Uniform}(0, 1)$ is independent of X_w, then $Y = X_w U^{1/\alpha} \sim \text{IHSB}(\alpha, \theta)$.

Proof. Conditionally on $X_w = x$, the random variable $Y \mid X_w = x$ has PDF

$$f_{Y|X_w}(y \mid x) = \alpha x^{-\alpha} y^{\alpha-1}, \quad 0 < y < x.$$

Integrating with respect to $f_{X_w}(x; \alpha, \theta)$, we obtain

$$f_Y(y; \alpha, \theta) = \int_y^\infty \alpha y^{\alpha-1} \frac{f(x; \theta)}{\mathbb{E}[X^\alpha]}\, dx = \frac{\alpha y^{\alpha-1} R(y; \theta)}{\mathbb{E}[X^\alpha]},$$

which coincides with the PDF in (2.1). □

This representation shows that the proposed IHSB family can be interpreted as a multiplicative Beta-type modulation of classical α-size-biased distributions. Specifically, the size-biasing step emphasizes large baseline observations, whereas the random contraction $U^{1/\alpha}$ introduces an inverse-hazard effect through the RF.

Based on Proposition 2, we propose Algorithm 1 for random variate generation. When the α-size-biased baseline admits a closed-form generator, random number generation from the IHSB model is straightforward and computationally efficient. This feature is particularly useful in practice, as it facilitates efficient Monte Carlo simulation and practical implementation of the proposed models.

Algorithm 1 Random variate generation for the IHSB family.

1: Generate X_w from the α-size-biased version of the baseline distribution.
2: Generate $U \sim \text{Unif}(0, 1)$.
3: Set $Y = X_w U^{1/\alpha}$.

2.3. Identifiability

The following result establishes the identifiability of the IHSB family under standard assumptions on the baseline distribution.

Proposition 3. *Let $g(x;\alpha,\theta)$ denote the PDF of the IHSB family given in Eq* (2.1)*. Assume that: (i) the baseline family is identifiable in θ; (ii) $\mathbb{E}_\theta(X^\alpha) < \infty$ for all admissible (α,θ); (iii) if, for some constants $c > 0$ and $d \in \mathbb{R}$, $R(x;\theta_1) = c\,x^d R(x;\theta_2)$ for all $x > 0$, then necessarily $d = 0$, $c = 1$, and $\theta_1 = \theta_2$.*

Then the parameter vector (α,θ) is identifiable; that is,

$$g(\cdot;\alpha_1,\theta_1) = g(\cdot;\alpha_2,\theta_2) \quad \text{a.e. on } (0,\infty) \quad \Longrightarrow \quad (\alpha_1,\theta_1) = (\alpha_2,\theta_2).$$

Proof. Suppose that

$$g(x;\alpha_1,\theta_1) = g(x;\alpha_2,\theta_2), \quad \forall x > 0.$$

By the definition of the IHSB density,

$$\frac{\alpha_1 x^{\alpha_1-1} R(x;\theta_1)}{E_{\theta_1}(X^{\alpha_1})} = \frac{\alpha_2 x^{\alpha_2-1} R(x;\theta_2)}{E_{\theta_2}(X^{\alpha_2})}, \quad \forall x > 0.$$

Rearranging terms, we obtain

$$R(x;\theta_1) = \left(\frac{\alpha_2 E_{\theta_1}(X^{\alpha_1})}{\alpha_1 E_{\theta_2}(X^{\alpha_2})}\right) x^{\alpha_2-\alpha_1} R(x;\theta_2) = c\,x^d R(x;\theta_2), \quad \forall x > 0,$$

where

$$c = \frac{\alpha_2 E_{\theta_1}(X^{\alpha_1})}{\alpha_1 E_{\theta_2}(X^{\alpha_2})} > 0, \quad d = \alpha_2 - \alpha_1.$$

By assumption (iii), it follows that $d = 0$, $c = 1$, and $\theta_1 = \theta_2$. Therefore, $\alpha_1 = \alpha_2$ and $\theta_1 = \theta_2$, which proves the identifiability of the parameter vector (α,θ). □

2.4. Reliability analysis

In this section, we present fundamental reliability measures associated with the IHSB distribution.

2.4.1. Reliability and hazard rate functions

The reliability and hazard rate functions are fundamental concepts in lifetime analysis, as they describe the operating behavior and risk of failure of engineering components and systems.

Proposition 4. *Let $X \sim \text{IHSB}(\alpha,\theta)$ denote the lifetime or time-to-failure of a component. The RF, defined as the probability that the component operates beyond time x, is given by*

$$R(x;\alpha,\theta) = \frac{\alpha\, m_\alpha(x;\theta)}{\mathbb{E}_\theta[X^\alpha]}, \quad x,\alpha > 0,$$

where

$$m_\alpha(x;\theta) = \int_x^\infty t^{\alpha-1} R(t;\theta)dt.$$

The corresponding HRF, which measures the instantaneous risk of failure at time x given survival up to that point, is expressed as

$$h(x) = \frac{x^{\alpha-1} R(x;\theta)}{m_\alpha(x;\theta)}, \quad x,\alpha > 0.$$

Proof. The result follows directly from the definition of the IHSB PDF and the standard forms of the RF and HRF. □

2.4.2. Mean time to failure

Another important reliability measure is the mean time to failure (MTTF), which represents the expected lifetime of a component before failure.

Proposition 5. *Let $X \sim \text{IHSB}(\alpha, \theta)$. Then MTTF is*

$$\text{MTTF} = \frac{\alpha}{\alpha + 1} \frac{\mathbb{E}_\theta[X^{\alpha+1}]}{\mathbb{E}_\theta[X^\alpha]}.$$

Proof. By definition of MTTF, and using the RF given in Proposition 4, we have that

$$\begin{aligned} \text{MTTF} &= \int_0^\infty R(x; \alpha, \theta) dx \\ &= \frac{\alpha}{\mathbb{E}_\theta[X^\alpha]} \int_0^\infty m_\alpha(x; \theta) dx \\ &= \frac{\alpha}{\mathbb{E}_\theta[X^\alpha]} \int_0^\infty t^\alpha R(t; \theta) dt, \end{aligned}$$

where the last equality follows from Tonelli–Fubini. Finally, using the moment identity

$$\mathbb{E}_\theta[X^r] = r \int_0^\infty t^{r-1} R(t; \theta) dt,$$

the result follows. □

2.4.3. Mean residual life

Proposition 6. *Let $X \sim \text{IHSB}(\alpha, \theta)$. Then, the mean residual life (MRL) function can be expressed as*

$$\text{MRL} = \frac{m_{\alpha+1}(x; \theta)}{m_\alpha(x; \theta)} - x,$$

where $m_{\alpha+j}(x; \theta)$, with $j = 0, 1$, is as in Proposition 4.

Proof. By definition of MRL, and using the RF given in Proposition 4, we have that

$$\begin{aligned} \text{MRL} &= \frac{1}{R(x; \alpha, \theta)} \int_x^\infty R(t; \alpha, \theta)\, dt \\ &= \frac{1}{m_\alpha(x; \theta)} \int_x^\infty m_\alpha(t; \theta)\, dt \\ &= \frac{1}{m_\alpha(x; \theta)} \int_x^\infty (u - x)\, u^{\alpha-1} R(u; \theta)\, du, \end{aligned}$$

where the last equality follows from Tonelli–Fubini. So, recognizing the function m_α in the integral of the last expression, the result follows. □

Remark 3. *Note that, as expected, the MRL generalizes the MTTF. In other words, by evaluating at $x = 0$, we obtain*

$$\mathrm{MRL}(0) = \frac{m_{\alpha+1}(0;\theta)}{m_{\alpha}(0;\theta)} = \frac{\alpha}{\alpha+1}\frac{\mathbb{E}_\theta[X^{\alpha+1}]}{\mathbb{E}_\theta[X^{\alpha}]} = \mathrm{MTTF}.$$

This result is consistent with the reliability interpretation, since at $x = 0$ the expected remaining lifetime coincides with the total expected lifetime of the component.

2.5. Moments

Proposition 7. *Let $X \sim \mathrm{IHSB}(\alpha, \theta)$. The r-th raw moment of X is*

$$\mathbb{E}(X^r) = \frac{\alpha}{\alpha+r}\frac{\mathbb{E}_\theta(X^{\alpha+r})}{\mathbb{E}_\theta(X^{\alpha})}, \quad r = 1, 2 \ldots. \tag{2.2}$$

Proof. From the PDF of the IHSB distribution,

$$\mathbb{E}(X^r) = \int_0^\infty x^r g(x;\alpha,\theta)\,dx = \frac{\alpha}{\mathbb{E}_\theta(X^{\alpha})}\int_0^\infty x^{\alpha+r-1}R(x;\theta)\,dx.$$

For a nonnegative random variable with RF $R(x;\theta)$, the identity

$$\mathbb{E}_\theta(X^k) = k\int_0^\infty x^{k-1}R(x;\theta)dx,\ k > 0$$

holds. Taking $k = \alpha + r$, we obtain

$$\int_0^\infty x^{\alpha+r-1}R(x;\theta)\,dx = \frac{1}{\alpha+r}\,\mathbb{E}_\theta(X^{\alpha+r}).$$

Substituting this expression into the previous integral, we obtain the desired result in (2.2). □

Corollary 1. *Let $X \sim \mathrm{IHSB}(\alpha, \theta)$. The mean ($\mathbb{E}(X)$) and variance ($\mathbb{V}(X)$) of X are given by*

$$\mathbb{E}(X) = \frac{\alpha\, m_1}{(\alpha+1)\, m_0}$$

and

$$\mathbb{V}(X) = \frac{\alpha}{m_0}\left[\frac{m_2}{\alpha+2} - \frac{\alpha\, m_1^2}{(\alpha+1)^2\, m_0}\right],$$

where $m_j = \mathbb{E}_\theta(X^{\alpha+j})$, $j = 0, 1, 2$.

Corollary 2. *Let $X \sim \mathrm{IHSB}(\alpha, \theta)$. Then, the Fisher coefficient of variation ($\mathbb{CV}(X)$), the Fisher skewness ($\mathbb{S}(X)$), and the Fisher kurtosis ($\mathbb{K}(X)$) of X are given by*

$$\mathbb{CV}(X) = \sqrt{\frac{(\alpha+1)^2}{\alpha(\alpha+2)}\frac{m_0\, m_2}{m_1^2} - 1},$$

$$\mathbb{S}(X) = \frac{\frac{m_3\, m_0^2}{\alpha+3} - \frac{3\,\alpha\, m_0\, m_1\, m_2}{(\alpha+1)(\alpha+2)} + \frac{2\alpha^2 m_1^3}{(\alpha+1)^3}}{\sqrt{\alpha}\left[\frac{m_2\, m_0}{\alpha+2} - \frac{\alpha\, m_1^2}{(\alpha+1)^2}\right]^{3/2}}$$

and

$$\mathbb{K}(X) = \frac{\frac{m_4\, m_0^3}{\alpha+4} - \frac{4\,\alpha\, m_1\, m_3\, m_0^2}{(\alpha+1)(\alpha+3)} + \frac{6\,\alpha^2\, m_1^2\, m_2\, m_0}{(\alpha+1)^2(\alpha+2)} - \frac{3\,\alpha^3\, m_1^4}{(\alpha+1)^4}}{\alpha\left[\frac{m_2\, m_0}{(\alpha+2)} - \frac{\alpha\, m_1^2}{(\alpha+1)^2}\right]^2},$$

where $m_{\alpha+j} = \mathbb{E}_\theta(X^{\alpha+j})$ *and* $j = 0, 1, 2, 3, 4$.

2.6. Some well-known special cases

This section illustrates representative members of the IHSB family obtained by using one-parameter baseline models such as the exponential, Rayleigh, and Pareto type II distributions.

2.6.1. Gamma distribution

Considering an exponential baseline distribution with reliability function $R(x;\beta) = e^{-x/\beta}$, $x, \beta > 0$, and using that its α-th moment is $\mathbb{E}(X^\alpha) = \beta^\alpha \Gamma(\alpha+1)$, $\alpha > 0$, Eq (2.1) reduces to

$$g(x;\alpha,\beta) = \frac{1}{\beta^\alpha \Gamma(\alpha)} x^{\alpha-1} e^{-\frac{x}{\beta}}, \quad x, \alpha, \beta > 0,$$

where

$$\Gamma(\alpha) = \int_0^\infty u^{\alpha-1} e^{-u} du$$

denotes the gamma function. This expression corresponds to the PDF of the gamma distribution with shape α and scale β (see [18]).

2.6.2. Generalized Rayleigh distribution

Considering a Rayleigh baseline distribution with reliability function $R(x;\theta) = e^{-\theta x^2}$, $x, \theta > 0$, and using that its α-th moment is

$$\mathbb{E}(X^\alpha) = \theta^{-\frac{\alpha}{2}} \Gamma\left(\tfrac{\alpha}{2}+1\right), \quad \alpha > 0,$$

Eq (2.1) reduces to

$$g(x;\alpha,\theta) = \frac{\alpha\, \theta^{\alpha/2}}{\Gamma\left(\frac{\alpha}{2}+1\right)} x^{\alpha-1} e^{-\theta x^2}, \quad x, \alpha, \theta > 0,$$

where $\Gamma(\cdot)$ denotes the gamma function. Under the parameterization $\alpha = 2k+2$, $k > 0$, this expression corresponds to the PDF of the generalized Rayleigh distribution (see [19]).

2.6.3. Beta prime distribution

Considering a Pareto type II (Lomax) baseline distribution with reliability function $R(x;\gamma) = (1 + x)^{-\gamma}$, $x, \gamma > 0$, and recalling that its α-th moment exists for $\alpha < \gamma$ and is given by

$$\mathbb{E}(X^\alpha) = \frac{\Gamma(\gamma - \alpha)\,\Gamma(\alpha + 1)}{\Gamma(\gamma)}, \quad 0 < \alpha < \gamma,$$

Eq (2.1) reduces to

$$g(x;\alpha,\gamma) = \frac{\Gamma(\gamma)}{\Gamma(\alpha)\,\Gamma(\gamma - \alpha)} x^{\alpha-1}(1 + x)^{-\gamma}, \quad x > 0,\ \gamma > \alpha > 0,$$

where $\Gamma(\cdot)$ denotes the gamma function. Under the parameterization $\gamma = a + b$ and $\alpha = a$, with $a, b > 0$, this expression corresponds to the PDF of the beta prime distribution (see [20]).

According to this result, the IHSB framework successfully reproduces several well-known two-parameter models, including the gamma, generalized Rayleigh, and beta prime distributions. These examples highlight the internal coherence and generality of the proposed family, confirming its ability to unify and extend classical lifetime distributions under a common formulation.

A summary of the baseline distributions and the corresponding models induced by the proposed IHSB construction is provided in Appendix B.

2.7. Two new special cases

This section introduces two new members of the IHSB family constructed from two one-parameter baseline distributions: the half-normal and Maxwell models.

2.7.1. IHSB half-normal distribution

Consider a half-normal baseline distribution [18] with RF:

$$R(x;\beta) = 2\left[1 - \Phi\left(\frac{x}{\beta}\right)\right],$$

for $x, \beta > 0$, where $\Phi(\cdot)$ denotes the standard normal CDF. The α-th non central moment is given by

$$\mathbb{E}_\beta(X^\alpha) = \frac{2^{\frac{\alpha}{2}}}{\sqrt{\pi}} \beta^\alpha \Gamma\left(\frac{\alpha + 1}{2}\right),$$

for $\alpha > 0$, where $\Gamma(\cdot)$ denotes the gamma function. Applying the IHSB transformation yields the IHSB half-normal (IHSBHN) distribution, whose PDF is

$$g(x;\alpha,\beta) = \frac{\sqrt{\pi}\,\alpha\, 2^{1-\frac{\alpha}{2}}}{\beta\,\Gamma(\frac{\alpha+1}{2})} \left(\frac{x}{\beta}\right)^{\alpha-1} \left[1 - \Phi\left(\frac{x}{\beta}\right)\right], \quad x, \alpha, \beta > 0. \tag{2.3}$$

From (2.3), it is clear that β acts as a scale parameter, whereas α controls the shape of the distribution. The distribution with PDF given by (2.3) is termed the IHSBHN distribution, and we write $X \sim \text{IHSBHN}(\alpha, \beta)$.

An explicit stochastic representation can be obtained for the IHSBHN distribution. Let $G \sim \text{Gamma}\left(\frac{\alpha+1}{2}, 1\right)$ and $U \sim \text{Uniform}(0,1)$ be independent random variables. Then,

$$X = \beta\sqrt{2G}\,U^{1/\alpha} \sim \text{IHSBHN}(\alpha,\beta). \tag{2.4}$$

This result follows directly from the general stochastic representation established in Section 2.2 and the fact that the α-size-biased version of the HN distribution admits the closed-form representation

$$X_w \overset{d}{=} \beta\sqrt{2G}.$$

Representation (2.4) is particularly useful from a computational perspective, as it provides an exact and efficient method for generating random variates from the IHSBHN distribution without requiring numerical inversion of the CDF or acceptance–rejection schemes.

The HRF of $X \sim \text{IHSBHN}(\alpha,\beta)$ is given by

$$h(x;\alpha,\beta) = \frac{2x^{\alpha-1}\left[1-\Phi\left(\frac{x}{\beta}\right)\right]}{m_{\text{HN}}(x)}, \quad x,\alpha,\beta > 0,$$

where

$$m_{\text{HN}}(x) = 2\int_x^\infty t^{\alpha-1}\left[1-\Phi\left(\frac{t}{\beta}\right)\right]dt.$$

Moreover, the r-th raw moment of X is given by

$$\mathbb{E}[X^r] = \frac{\alpha}{\alpha+r}\frac{2^{r/2}\beta^r\,\Gamma\left(\frac{\alpha+r+1}{2}\right)}{\Gamma\left(\frac{\alpha+1}{2}\right)}, \quad r = 1,2,3,\ldots,$$

and, consequently, the skewness and kurtosis coefficients are computed using Corollary 2.

Figure 1 illustrates the behavior of the PDF and the HRF of the IHSBHN distribution for $\beta = 1$ and different values of α. The plots show that the PDF may exhibit decreasing or unimodal shapes, whereas the HRF can display both monotone and non-monotone patterns depending on the value of α, including decreasing, increasing, and bathtub-shaped behaviors. Figure 2 depicts the behavior of the skewness and kurtosis of the IHSBHN distribution, indicating that larger values of both measures are attained for smaller values of α.

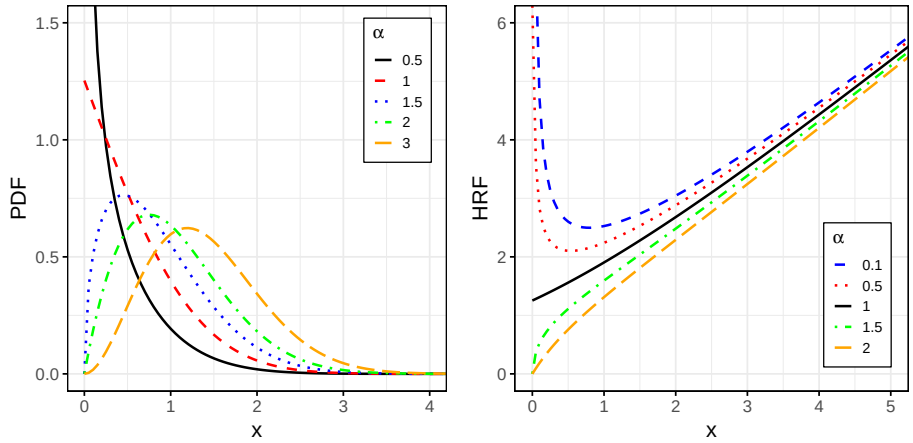

Figure 1. PDF and HRF curves of the IHSBHN distribution for $\beta = 1$ and different values of α.

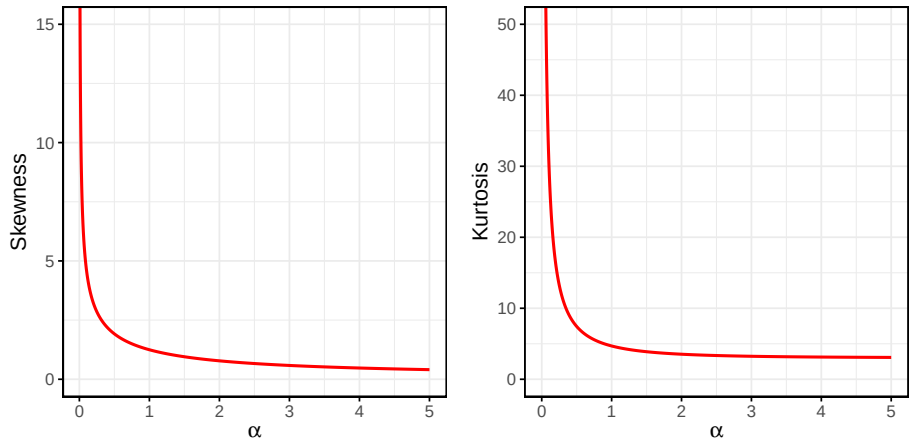

Figure 2. Skewness and kurtosis coefficients curves of the IHSBHN distribution.

2.7.2. IHSB Maxwell distribution

Consider a Maxwell (M) baseline distribution with RF

$$R(x;\beta) = \frac{2}{\sqrt{\pi}}\Gamma\left(\frac{3}{2}, \frac{x^2}{2\beta^2}\right), \quad x, \beta > 0,$$

where

$$\Gamma(a, x) = \int_x^\infty u^{a-1}e^{-u}du,$$

for $a > 0$, denotes the upper incomplete gamma function [18]. The α-th non-central moment is given by

$$\mathbb{E}_\beta[X^\alpha] = \frac{2^{\frac{\alpha}{2}+1}}{\sqrt{\pi}}\beta^\alpha\,\Gamma\left(\tfrac{\alpha+3}{2}\right), \quad \alpha > 0,$$

where $\Gamma(\cdot)$ denotes the gamma function.

Applying the IHSB transformation yields the IHSB Maxwell (IHSBM) distribution, whose PDF is

$$g(x;\alpha,\beta) = \frac{\alpha}{2^{\frac{\alpha}{2}}\,\Gamma\left(\frac{\alpha+3}{2}\right)\beta}\left(\frac{x}{\beta}\right)^{\alpha-1}\Gamma\left(\frac{3}{2}, \frac{1}{2}\left[\frac{x}{\beta}\right]^2\right), \quad x, \beta, \alpha > 0. \tag{2.5}$$

From (2.5), it follows that β acts as a scale parameter, while α controls the shape of the distribution. We denote this model by $X \sim \text{IHSBM}(\alpha, \beta)$.

In contrast to the HN case, the polynomial structure of the M PDF induces a different α-size-biased component. Specifically, let $G \sim \text{Gamma}\left(\frac{\alpha+3}{2}, 1\right)$ and $U \sim \text{Uniform}(0, 1)$ be independent random variables. Then,

$$X = \beta\sqrt{2G}\,U^{1/\alpha} \sim \text{IHSBM}(\alpha, \beta). \tag{2.6}$$

This representation follows directly from the general result established in Section 2.2 and highlights how the additional quadratic term in the M baseline modifies the latent gamma component relative to the IHSBHN case. From a computational perspective, representation (2.6) provides an exact and efficient mechanism for generating random variates from the IHSBM distribution.

The HRF of $X \sim \text{IHSBM}(\alpha, \beta)$ is given by

$$h(x;\alpha,\beta) = \frac{2x^{\alpha-1}\Gamma\left(\frac{3}{2}, \frac{x^2}{2\beta^2}\right)}{\sqrt{\pi}\, m_{\text{M}}(x)}, \quad x, \alpha, \beta > 0,$$

where

$$m_{\text{M}}(x;\beta) = \frac{2}{\sqrt{\pi}} \int_x^{\infty} t^{\alpha-1}\Gamma\left(\frac{3}{2}, \frac{t^2}{2\beta^2}\right) dt.$$

The r-th raw moment of X is given by

$$\mathbb{E}[X^r] = \frac{\alpha}{\alpha + r} 2^{\frac{r}{2}} \beta^r \frac{\Gamma(\frac{\alpha+r+3}{2})}{\Gamma(\frac{\alpha+3}{2})}, \quad r = 1, 2, 3, \ldots,$$

and the skewness and kurtosis coefficients follow directly from Corollary 2.

Figure 3 illustrates the behavior of the PDF and the HRF of the IHSBM distribution for $\beta = 1$ and different values of α. The plots show that the PDF may exhibit decreasing or unimodal shapes, whereas the HRF can display both monotone and non monotone patterns depending on the value of α, including decreasing, increasing, and bathtub-shaped behaviors. Figure 4 depicts the behavior of the skewness and kurtosis of the IHSBM distribution as functions of the shape parameter α, indicating that larger values of both measures are attained for smaller values of α.

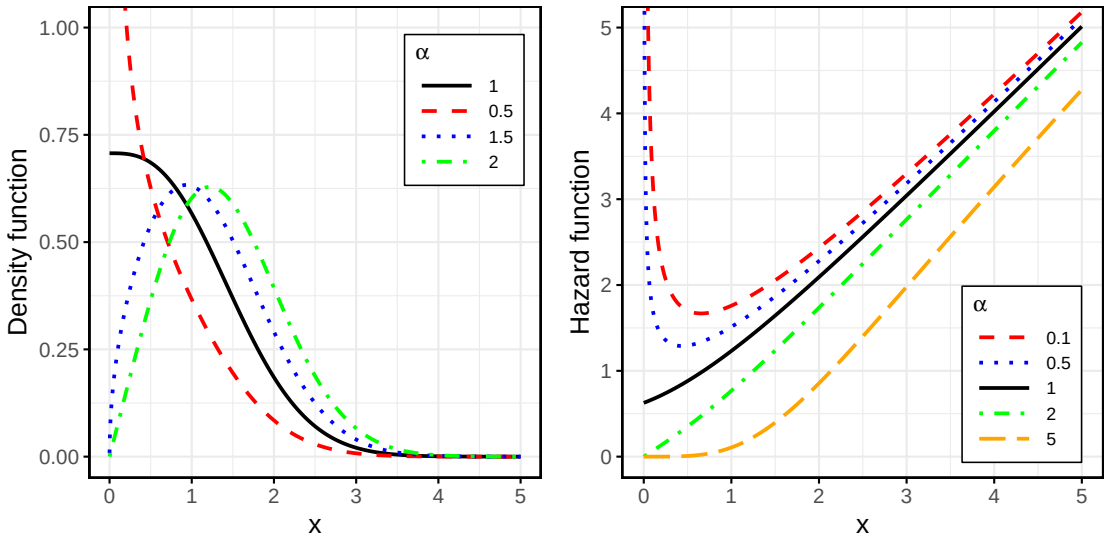

Figure 3. PDF and HRF curves of the IHSBM distribution for $\beta = 1$ and different values of α.

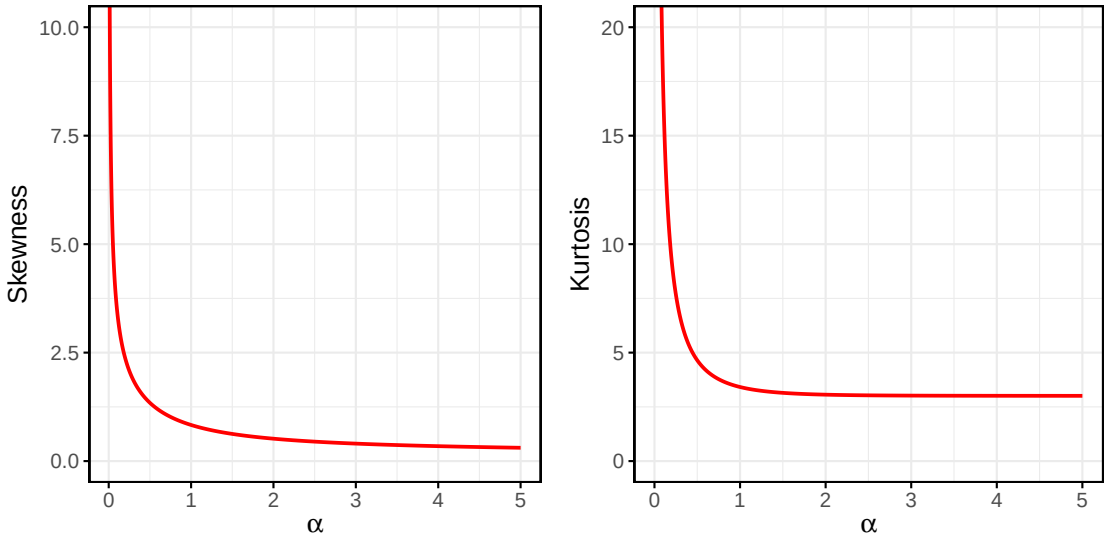

Figure 4. Skewness and kurtosis coefficients curves of the IHSBM distribution.

A computational implementation with graphical illustrations for the IHSBHN and IHSBM models is provided in scripts 01 and 04 of the repository reported in Section 1.

A consolidated summary of the baseline distributions and the corresponding models induced by the proposed IHSB construction, including the newly introduced IHSBHN and IHSBM distributions, is provided in Appendix B (see Table 10).

3. Parameter estimation

In this section, we analyze parameter estimation for the IHSB distributions, focusing on the method of moments and maximum likelihood estimation. To assess the performance of these estimators, a Monte Carlo simulation study is conducted, examining their empirical properties under different scenarios.

3.1. Moment estimation

Let $X_1, X_2, \ldots, X_n$ be a random sample from the distribution $X \sim \text{IHSB}(\alpha, \theta)$, where $\theta = (\theta_1, \theta_2, \ldots, \theta_k)^\top$, with $k \in \mathbb{N}$. The method-of-moments estimator of $\delta = (\alpha, \theta)^\top$ is defined as the solution of the system of equations

$$\frac{\hat{\alpha}_{\text{M}}}{\hat{\alpha}_{\text{M}} + j} \frac{\mathbb{E}_\theta\left(X^{\hat{\alpha}_{\text{M}}+j}\right)}{\mathbb{E}_\theta(X^{\hat{\alpha}_{\text{M}}})} - \overline{X^j} = 0, \qquad j = 1, 2, \ldots, k+1, \tag{3.1}$$

where $\mathbb{E}_\theta(X^{\hat{\alpha}_{\text{M}}})$ and $\mathbb{E}_\theta(X^{\hat{\alpha}_{\text{M}}+j})$ denote the theoretical moments of orders $\hat{\alpha}_{\text{M}}$ and $\hat{\alpha}_{\text{M}} + j$ under the baseline model indexed by θ, and $\overline{X^j}$ represents the sample mean of the jth power of the observations.

For the special cases IHSBHN and IHSBM discussed in Section 2.7, the moment estimator $\hat{\alpha}_{\text{M}}$ of α satisfies the scalar equation

$$a_1(\hat{\alpha}_{\text{M}})\,\overline{X}^2 - a_2(\hat{\alpha}_{\text{M}})\,\overline{X^2} = 0, \tag{3.2}$$

where $\overline{X}$ denotes the sample mean and $\overline{X^2}$ is the sample mean of the squared observations. The functions $a_1(\cdot)$ and $a_2(\cdot)$ are reported in Table 1.

Table 1. Functions involved in the moment estimation for the IHSBHN and IHSBM distributions.

Function	IHSBHN	IHSBM
$a_1(\alpha)$	$(\alpha+1)^3\Gamma^2(\frac{\alpha+1}{2})$	$(\alpha+1)^2(\alpha+3)\Gamma^2(\frac{\alpha+3}{2})$
$a_2(\alpha)$	$2\alpha(\alpha+2)\Gamma^2(\frac{\alpha+2}{2})$	$2\alpha(\alpha+2)\Gamma^2(\frac{\alpha+4}{2})$
$a_3(\alpha)$	$\frac{(\alpha+1)\Gamma(\frac{\alpha+1}{2})}{\sqrt{2}\alpha\Gamma(\frac{\alpha+2}{2})}$	$\frac{(\alpha+1)\Gamma(\frac{\alpha+3}{2})}{\sqrt{2}\alpha\Gamma(\frac{\alpha+4}{2})}$

In this work, we employ the `uniroot.all()` function from the `rootSolve` package in the R software environment [21, 22] to solve Eq (3.2). Once $\hat{\alpha}_{\mathrm{M}}$ has been computed, the moment estimator of the scale parameter β is given by $\hat{\beta}_{\mathrm{M}} = a_3(\hat{\alpha}_{\mathrm{M}})\,\overline{X}$, where the function $a_3(\cdot)$ is also reported in Table 1.

3.2. Maximum likelihood estimation

Let $X_1, X_2, \ldots, X_n$ be a random sample of size n from $X \sim \mathrm{IHSB}(\alpha, \theta)$, where $\theta = (\theta_1, \theta_2, \ldots, \theta_k)^\top$, with $k \in \mathbb{N}$. The log-likelihood function associated with $\delta = (\alpha, \theta^\top)^\top$ is written as

$$\begin{aligned}\ell(\delta; x_i) &= \log \prod_{i=1}^{n} \frac{\alpha\, x_i^{\alpha-1} R(x_i;\theta)}{\mathbb{E}_\theta[X^\alpha]} \\ &= n\log\alpha + (\alpha-1)\sum_{i=1}^{n}\log x_i + \sum_{i=1}^{n}\log R(x_i;\theta) - n\log\mathbb{E}_\theta[X^\alpha], \end{aligned} \tag{3.3}$$

where $\mathbb{E}_\theta[X^\alpha]$ denotes the moment of order α under the baseline model indexed by θ.

The score equations are given by

$$U_\alpha = \frac{\partial\ell(\delta; x_i)}{\partial\alpha} = \frac{n}{\alpha} + \sum_{i=1}^{n}\log(x_i) - n\frac{\mathbb{E}_\theta[X^\alpha\log(X)]}{\mathbb{E}_\theta[X^\alpha]} = 0, \tag{3.4}$$

$$U_{\theta_j} = \frac{\partial\ell(\delta; x_i)}{\partial\theta_j} = \sum_{i=1}^{n}\frac{1}{R(x_i;\theta)}\frac{\partial R(x_i;\theta)}{\partial\theta_j} - \frac{n}{\mathbb{E}_\theta[X^\alpha]}\frac{\partial\mathbb{E}_\theta[X^\alpha]}{\partial\theta_j} = 0, \tag{3.5}$$

for $j = 1, 2, \ldots, k$.

The maximum likelihood estimator $\hat{\delta}_{\mathrm{ML}} = (\hat{\alpha}_{\mathrm{ML}}, \hat{\theta}_{\mathrm{ML}}^\top)^\top$ de $\delta = (\alpha, \theta^\top)^\top$ is obtained by solving the system of Eqs (3.4) and (3.5) with respect to α and θ. Since this system does not admit a closed-form solution, the estimates must be obtained using numerical methods.

Approximate standard errors for $\hat{\delta}_{\mathrm{ML}}$ can be obtained from the inverse of the observed information matrix evaluated at $\hat{\delta}_{\mathrm{ML}}$. Specifically, let $H(\delta) = \frac{\partial^2\ell(\delta;\mathbf{x})}{\partial\delta\,\partial\delta^\top}$ denote the Hessian matrix of the log-likelihood, where $\delta = (\alpha, \theta^\top)^\top$. The observed information matrix is defined as $J(\delta) = -H(\delta)$, and the asymptotic covariance matrix of $\hat{\delta}_{\mathrm{ML}}$ is approximated by $\widehat{\mathrm{cov}}(\hat{\delta}_{\mathrm{ML}}) = J(\hat{\delta}_{\mathrm{ML}})^{-1}$. Therefore, the standard error of each component of $\hat{\delta}_{\mathrm{ML}}$ is given by the square root of the corresponding diagonal entry of $\widehat{\mathrm{cov}}(\hat{\delta}_{\mathrm{ML}})$.

In this work, we use the `optim()` function from the R software environment to compute $\hat{\delta}_{\mathrm{ML}}$ by maximizing (3.3). This function provides a numerical approximation of the Hessian matrix which is used to obtain the corresponding standard errors. In particular, we employ the L-BFGS-B method [23], a limited-memory quasi-Newton algorithm that approximates the Hessian using gradient information and allows box constraints on the parameter space, making it especially suitable for enforcing parameter positivity. For the special cases IHSBHN and IHSBM discussed in Section 2.7, the moment estimates were used as initial values for the iterative optimization procedure.

3.3. Simulation study

In this section, we conduct a Monte Carlo simulation study to evaluate the finite-sample performance of the method-of-moments and maximum likelihood estimators for the parameters of the IHSBHN and IHSBM distributions.

We generated 1000 random samples of sizes $n = 50, 100, 200, 300$, and 400 from these distributions using their stochastic representations, which led to the random generation procedure summarized in Algorithm 2.

Algorithm 2 Random generation from the IHSBHN / IHSBM distribution.

Require: Shape parameter $\alpha > 0$ and scale parameter $\beta > 0$
Ensure: A random variate $X \sim \mathrm{IHSBHN}(\alpha, \beta)$ or $X \sim \mathrm{IHSBM}(\alpha, \beta)$
1: Generate $G \sim \mathrm{Gamma}\left(\frac{\alpha+1}{2}, 1\right)$ for IHSBHN model or $G \sim \mathrm{Gamma}\left(\frac{\alpha+3}{2}, 1\right)$ for IHSBM model
2: Generate $U \sim \mathrm{Uniform}(0, 1)$
3: Set $X \leftarrow \beta \sqrt{2G}\, U^{1/\alpha}$
4: **return** X

Four simulation scenarios were considered. The values of the shape parameter α were selected to represent different distributional regimes in terms of kurtosis, ranging from strongly leptokurtic to near-mesokurtic behavior. Specifically, we considered $\alpha \in \{0.1, 0.5, 1, 10\}$. The scale parameter β was varied to reflect different scaling levels of the distribution. In particular, we considered $\beta \in \{2, 4, 8, 12\}$.

This design allows us to evaluate the performance of the proposed estimators under a wide range of distributional shapes and scaling levels. The scenarios are summarized in Table 2 as follows:

Table 2. Simulation scenarios considered in the Monte Carlo study.

Scenario	α	β	Kurtosis regime	Scaling level
A	0.1	2	Strongly leptokurtic	Low
B	0.5	4	Moderately leptokurtic	Moderate
C	1	8	Mildly leptokurtic	High
D	10	12	Near-mesokurtic	Very high

For each generated sample, we computed the moment and maximum likelihood estimates, $(\hat{\alpha}_{\mathrm{M}}, \hat{\beta}_{\mathrm{M}})^{\top}$ and $(\hat{\alpha}_{\mathrm{ML}}, \hat{\beta}_{\mathrm{ML}})^{\top}$, respectively, following the computational procedures described in Sections 3.1 and 3.2 (Script 05 of the repository reported in Section 1 provides details on the R code used). Based on these estimates, the following performance measures were evaluated. For brevity, the definitions are presented for the parameter α, and analogous measures were computed for β.

i. *Average estimates*: $\overline{\hat{\alpha}_{\mathrm{M}}} = \frac{1}{1000}\sum_{i=1}^{1000}\hat{\alpha}_{\mathrm{M}_i}$.

ii. *Standard deviations*: $\mathrm{sd}(\hat{\alpha}_{\mathrm{M}}) = \sqrt{\frac{1}{999}\sum_{i=1}^{1000}(\hat{\alpha}_{\mathrm{M}_i} - \overline{\hat{\alpha}_{\mathrm{M}}})^2}$.

For the maximum likelihood estimators, the same measures were computed, and additionally the average standard errors were evaluated as $\mathrm{se}(\hat{\alpha}_{\mathrm{ML}}) = \frac{1}{1000}\sum_{i=1}^{1000}\mathrm{se}(\hat{\alpha}_{\mathrm{ML}_i})$, where $\mathrm{se}(\hat{\alpha}_{\mathrm{ML}_i})$ is obtained from the observed information matrix associated with the ith generated sample.

Tables 3 and 4 summarize the results of the Monte Carlo simulation study for the different scenarios and sample sizes. Overall, the average parameter estimates are close to the true values, with this agreement improving as the sample size increases. In addition, the standard deviations of the estimators decrease as n grows, providing empirical evidence of the consistency of both the method-of-moments and maximum likelihood estimators.

When comparing the two estimation methods, the maximum likelihood approach generally yields smaller standard deviations than those obtained via the method of moments, indicating greater efficiency across the analyzed scenarios. Finally, for the maximum likelihood method, a close agreement is observed between the empirical standard deviations and the average standard errors derived from the observed information matrix, suggesting that the asymptotic variance approximation performs well even for moderate sample sizes.

Table 3. Monte Carlo simulation results for the IHSBHN distribution.

Scenario	n	$\overline{\hat{\alpha}_{\mathrm{M}}}$	$\mathrm{sd}(\hat{\alpha}_{\mathrm{M}})$	$\overline{\hat{\beta}_{\mathrm{M}}}$	$\mathrm{sd}(\hat{\beta}_{\mathrm{M}})$	$\overline{\hat{\alpha}_{\mathrm{ML}}}$	$\mathrm{sd}(\hat{\alpha}_{\mathrm{ML}})$	$\mathrm{se}(\hat{\alpha}_{\mathrm{ML}})$	$\overline{\hat{\beta}_{\mathrm{ML}}}$	$\mathrm{sd}(\hat{\beta}_{\mathrm{ML}})$	$\mathrm{se}(\hat{\beta}_{\mathrm{ML}})$
A	50	0.125	0.042	1.779	0.855	0.104	0.016	0.015	1.910	0.777	0.751
	100	0.111	0.029	1.884	0.626	0.102	0.010	0.010	1.942	0.548	0.538
	200	0.107	0.021	1.940	0.465	0.101	0.007	0.007	1.977	0.379	0.386
	300	0.104	0.017	1.956	0.371	0.100	0.006	0.006	1.977	0.307	0.315
	400	0.103	0.015	1.983	0.346	0.101	0.005	0.005	1.990	0.275	0.274
B	50	0.543	0.121	3.841	0.866	0.524	0.084	0.082	3.878	0.760	0.752
	100	0.521	0.082	3.917	0.616	0.511	0.058	0.056	3.939	0.532	0.541
	200	0.511	0.060	3.974	0.465	0.505	0.040	0.039	3.988	0.399	0.388
	300	0.507	0.047	3.973	0.367	0.503	0.032	0.032	3.980	0.319	0.316
	400	0.507	0.042	3.993	0.328	0.503	0.027	0.028	3.996	0.274	0.275
C	50	1.058	0.218	7.820	1.322	1.051	0.181	0.170	7.800	1.173	1.196
	100	1.028	0.142	7.912	0.945	1.021	0.121	0.117	7.926	0.884	0.862
	200	1.013	0.101	7.972	0.670	1.010	0.084	0.082	7.972	0.602	0.613
	300	1.010	0.082	7.968	0.552	1.006	0.069	0.066	7.979	0.508	0.501
	400	1.010	0.070	7.946	0.481	1.005	0.058	0.058	7.985	0.433	0.432
D	50	10.546	2.034	11.856	1.256	10.546	2.024	1.941	11.855	1.254	1.235
	100	10.286	1.396	11.905	0.914	10.288	1.393	1.337	11.903	0.908	0.877
	200	10.128	0.927	11.950	0.611	10.128	0.913	0.930	11.950	0.606	0.623
	300	10.106	0.755	11.966	0.505	10.104	0.747	0.757	11.967	0.500	0.509
	400	10.058	0.671	11.988	0.458	10.062	0.664	0.653	11.985	0.453	0.441

Table 4. Monte Carlo simulation results for the IHSBM distribution.

Scenario	n	$\overline{\hat{\alpha}_{\mathrm{M}}}$	sd($\hat{\alpha}_{\mathrm{M}}$)	$\overline{\hat{\beta}_{\mathrm{M}}}$	sd($\hat{\beta}_{\mathrm{M}}$)	$\overline{\hat{\alpha}_{\mathrm{ML}}}$	sd($\hat{\alpha}_{\mathrm{ML}}$)	se($\hat{\alpha}_{\mathrm{ML}}$)	$\overline{\hat{\beta}_{\mathrm{ML}}}$	sd($\hat{\beta}_{\mathrm{ML}}$)	se($\hat{\beta}_{\mathrm{ML}}$)
A	50	0.112	0.035	1.844	0.576	0.103	0.016	0.015	1.862	0.542	0.542
	100	0.107	0.026	1.938	0.450	0.102	0.011	0.010	1.944	0.407	0.401
	200	0.103	0.017	1.983	0.325	0.101	0.008	0.007	1.987	0.302	0.290
	300	0.102	0.014	1.983	0.257	0.101	0.006	0.006	1.986	0.237	0.237
	400	0.101	0.012	1.985	0.216	0.101	0.005	0.005	1.987	0.205	0.205
B	50	0.531	0.110	3.928	0.619	0.523	0.087	0.081	3.931	0.582	0.564
	100	0.512	0.073	3.970	0.430	0.508	0.055	0.056	3.974	0.398	0.405
	200	0.508	0.051	3.974	0.299	0.507	0.038	0.039	3.975	0.278	0.286
	300	0.506	0.042	3.988	0.251	0.504	0.033	0.032	3.990	0.235	0.235
	400	0.502	0.036	3.998	0.215	0.501	0.027	0.027	3.999	0.203	0.204
C	50	1.057	0.212	7.896	1.007	1.048	0.187	0.174	7.905	0.959	0.910
	100	1.023	0.138	7.960	0.694	1.015	0.118	0.118	7.977	0.658	0.650
	200	1.014	0.097	7.961	0.487	1.010	0.082	0.083	7.979	0.464	0.459
	300	1.011	0.079	7.970	0.417	1.009	0.069	0.068	7.983	0.400	0.375
	400	1.007	0.067	7.984	0.338	1.005	0.060	0.058	7.989	0.319	0.325
D	50	10.627	2.257	11.810	1.160	10.617	2.249	2.153	11.814	1.154	1.175
	100	10.306	1.588	11.909	0.874	10.306	1.567	1.477	11.907	0.861	0.837
	200	10.191	1.026	11.942	0.582	10.191	1.017	1.033	11.942	0.580	0.594
	300	10.083	0.850	11.972	0.491	10.080	0.840	0.834	11.973	0.486	0.486
	400	10.060	0.697	11.987	0.400	10.061	0.691	0.721	11.986	0.396	0.421

4. Data analysis

In this section, we illustrate the practical usefulness of the IHSB distributions by fitting the two special cases IHSBHN and IHSBM to two real data sets arising from engineering-related contexts. For comparison purposes, we also consider the gamma (G), Weibull (W), log-normal (LN), and generalized exponential (GE) distributions [18, 24, 25], which are commonly used to model this type of data and involve the same number of parameters as the fitted IHSB distributions. The PDFs and RFs of this distributions are presented in Table 5.

The goodness of fit is assessed using the Cramér–von Mises (CvM) and Anderson–Darling (AD) tests [26], while the Akaike information criterion (AIC) (Akaike [27]) and the Bayesian information criterion (BIC) (Schwarz [28]) are employed to evaluate the comparative performance of the competing models.

The R codes employed in the present analysis are provided in scripts 07 and 08 within the repository reported in Section 1.

Table 5. PDFs and RFs of common positive support distributions.

Distribution	PDF	RF
G	$\frac{1}{\Gamma(\alpha)\beta^{\alpha}}x^{\alpha-1}e^{-x/\beta}$	$\frac{\Gamma(\alpha,\ x/\beta)}{\Gamma(\alpha)}$
W	$\frac{\alpha}{\beta}\left(\frac{x}{\beta}\right)^{\alpha-1}\exp\left[-\left(\frac{x}{\beta}\right)^{\alpha}\right]$	$\exp\left[-\left(\frac{x}{\beta}\right)^{\alpha}\right]$
LN	$\frac{1}{x\beta\sqrt{2\pi}}\exp\left[-\frac{(\log x-\alpha)^2}{2\beta^2}\right]$	$1-\Phi\left(\frac{\log x-\alpha}{\beta}\right)$
GE	$\frac{\alpha}{\beta}e^{-\frac{x}{\beta}}\left(1-e^{-\frac{x}{\beta}}\right)^{\alpha-1}$	$1-\left(1-e^{-\frac{x}{\beta}}\right)^{\alpha}$

Note: For all distributions, $x, \alpha, \beta > 0$. Here, $\Gamma(\cdot)$ denotes the complete gamma function, $\Gamma(a) = \int_0^{\infty} t^{a-1}e^{-t}\,dt$ for $a > 0$, and $\Gamma(a,u)$ denotes the upper incomplete gamma function, $\Gamma(a,u) = \int_u^{\infty} t^{a-1}e^{-t}\,dt$ for $u, a > 0$.

4.1. Fatigue life data

The data consist of 100 observations on fatigue life, measured in cycles $\times 10^{-3}$, corresponding to 6061–T6 aluminum coupons tested under a maximum stress of 31,000 psi per cycle, as reported in [29]. Table 6 reports some descriptive statistics of the fatigue life data. In particular, the data exhibit moderate skewness and a leptokurtic behavior, which is influenced by the presence of outlying observations. This pattern is clearly illustrated in Figure 5, which also suggests a unimodal structure in the data distribution.

Table 6. Descriptive statistics of fatigue life data.

Sample size	Minimun	Maximum	Mean	Variance	Skewness	Kurtosis
100	5.000	147.000	68.340	502.631	0.409	4.252

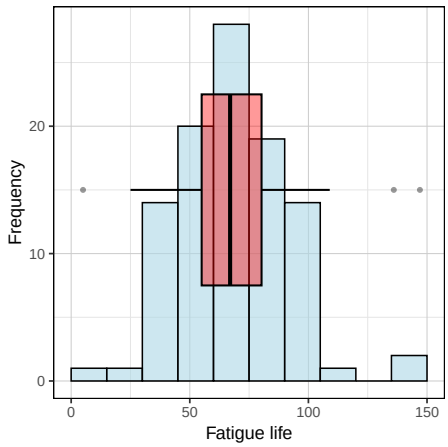

Figure 5. Histogram and boxplot for the fatigue life data.

Table 7 reports the maximum likelihood estimates of the model parameters (with standard errors in parentheses), along with the results of goodness-of-fit tests and the corresponding information criteria.

Overall, the IHSBM distribution yields the lowest AIC and BIC values and comparatively larger p-values in the goodness-of-fit tests, indicating an improved fit relative to the competing models.

Table 7. Maximum likelihood estimates (standard errors in parentheses), goodness-of-fit statistics (p-value in parentheses), and information criteria for the fitted models.

Parameter	IHSBM	W	G	LN	GE
α	4.177	3.210	7.683	4.158	9.676
	(0.571)	(0.237)	(1.064)	(0.041)	(1.844)
β	32.618	75.923	8.895	0.411	24.174
	(2.260)	(2.491)	(1.273)	(0.029)	(1.924)
AD	0.524	0.665	0.664	2.245	2.138
	(0.722)	(0.588)	(0.589)	(0.068)	(0.077)
CvM	0.078	0.090	0.103	0.367	0.341
	(0.705)	(0.635)	(0.569)	(0.088)	(0.104)
AIC	911.5	912.6	919.8	941.7	931.8
BIC	916.8	917.8	925.0	946.9	937.1

Figure 6 displays the fitted PDFs (left panel) and the corresponding hazard rate functions (right panel). The IHSBM PDF closely follows the empirical distribution of the data, adequately capturing its skewness and unimodal shape. In terms of hazard behavior, the IHSBM model exhibits a pattern clearly distinct from the classical distributions, particularly for larger fatigue life values. Notably, its hazard rate lies between those of the G and W models, reflecting additional flexibility in modeling the tail risk. This improved performance can be attributed to the weighting mechanism of the IHSB model, which assigns greater probability mass to observations associated with lower hazard rates. In the context of fatigue life data, this allows the model to provide a more balanced representation of the right tail, avoiding the overestimation or underestimation exhibited by some classical models, while maintaining a good fit in the central region.

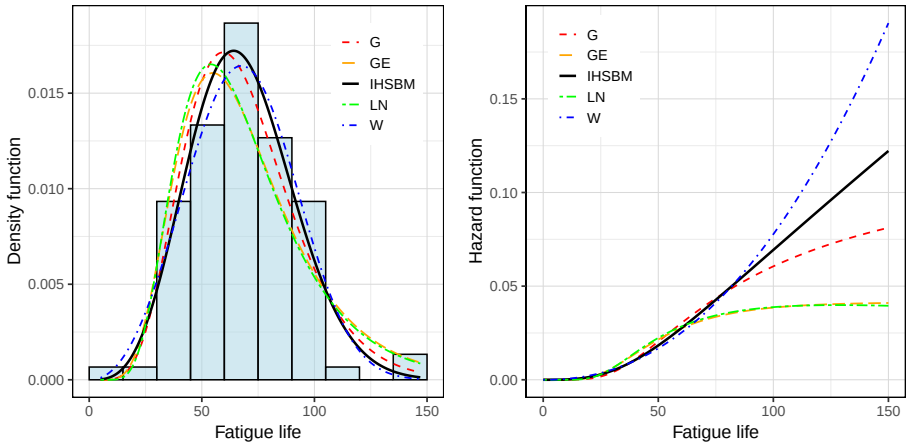

Figure 6. Histogram of the fatigue life data with fitted PDFs (left panel) and the corresponding HRFs for the IHSBM, G, W, LN, and GE distributions (right panel).

4.2. Tensile strength data

This data set consists of 69 observations of tensile strength, measured in GPa, obtained from carbon fiber specimens tested under tension with a gauge length of 20 mm [30]. Basic descriptive statistics are reported in Table 8. In contrast to the fatigue life data, the tensile strength measurements exhibit an approximately symmetric distribution with mild kurtosis, as also suggested by the histogram and boxplot displayed in Figure 7.

Table 8. Descriptive statistics of fatigue life data.

Sample size	Minimun	Maximum	Mean	Variance	Skewness	Kurtosis
69	1.312	3.585	2.451	0.245	-0.028	2.941

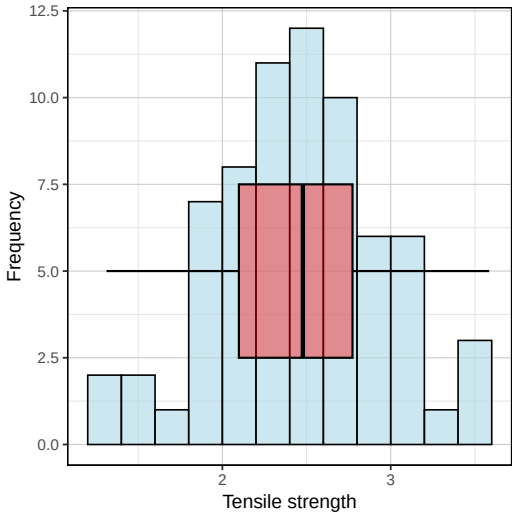

Figure 7. Histogram and boxplot for the tensile strength data.

Table 9 summarizes the maximum likelihood estimates, goodness-of-fit statistics, and information criteria for the fitted models. Among the competing distributions, the IHSBHN model achieves the lowest AIC and BIC values and exhibits the largest p-values in the AD and CvM tests, indicating a superior overall fit for this data set.

Figure 8 presents the fitted PDFs and the corresponding HRFs. The IHSBHN distribution closely matches the empirical density and provides a flexible hazard rate shape, further supporting its suitability for modeling tensile strength data. The improved fit can be explained by the additional flexibility introduced by the inverse-hazard weighting mechanism, which allows the model to adapt to the overall shape of the data while maintaining a realistic hazard rate behavior. This is particularly relevant for tensile strength data, where classical models may impose restrictive hazard structures that do not fully reflect the underlying failure mechanism.

Table 9. Maximum likelihood estimates (standard errors in parentheses), goodness-of-fit statistics (p-value in parentheses), and information criteria for the fitted models.

Parameter	IHSBHN	W	G	LN	GE
α	13.204	5.505	23.317	0.875	88.2180
	(2.093)	(0.501)	(3.909)	(0.026)	(33.342)
β	0.712	2.651	0.105	0.212	0.491
	(0.062)	(0.061)	(0.018)	(0.018)	(0.044)
AD	0.210	0.274	0.335	0.544	1.120
	(0.988)	(0.956)	(0.909)	(0.701)	(0.300)
CvM	0.026	0.034	0.045	0.076	0.160
	(0.988)	(0.961)	(0.907)	(0.714)	0.362
AIC	102.496	103.192	104.075	106.768	113.240
BIC	106.964	107.661	108.543	111.237	117.709

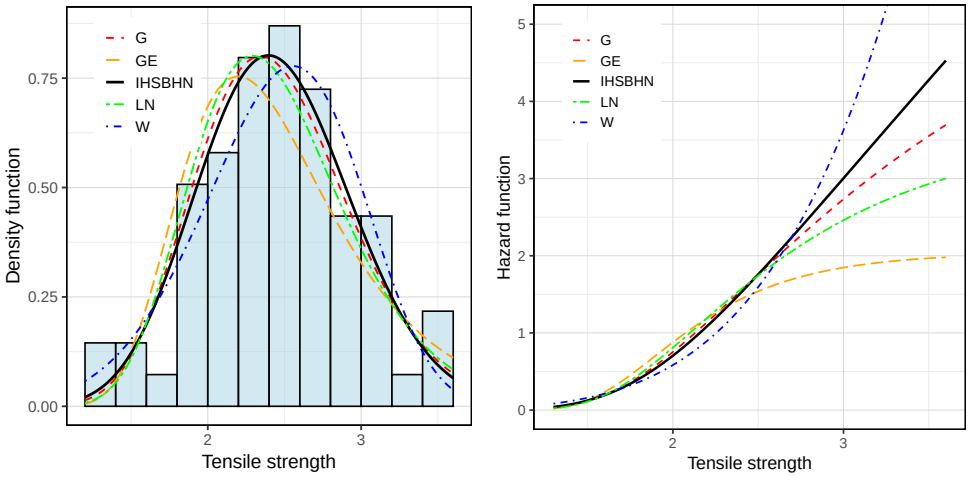

Figure 8. Histogram of the tensile strength data with fitted PDFs (left panel) and the corresponding HRFs for the IHSBM, G, W, LN, and GE distributions (right panel).

5. Concluding remarks

This paper introduced a new family of weighted distributions, referred to as the IHSB family, providing a unified and interpretable framework for constructing flexible lifetime models. The proposed IHSB formulation is conceptually related to classical size-biased schemes, while introducing a distinct weighting mechanism that explicitly incorporates reliability information through the hazard rate of the baseline distribution. In this way, the proposed approach establishes a direct link between weighted distribution theory and fundamental concepts from reliability analysis.

Several distributional properties of the proposed IHSB family were derived, including reliability measures, moments, and inferential characteristics. The framework was shown to reproduce a number of well-known distributions from the literature as particular constructions within the proposed mechanism, while also generating new models based on half-normal and Maxwell baseline

distributions, namely the IHSBHN and IHSBM distributions. These new cases admit PDFs with monotone decreasing or unimodal shapes, together with HRFs that can be monotone increasing or initially decreasing and subsequently increasing, yielding asymmetric U-shaped patterns.

Parameter estimation for the IHSB family and its special cases was addressed using the method of moments and maximum likelihood. A Monte Carlo simulation study demonstrated that both estimation procedures perform satisfactorily in finite samples, with the maximum likelihood estimator showing improved efficiency and accurate standard error approximations even for moderate sample sizes. The practical relevance of the proposed models was further illustrated through real data applications from engineering contexts, where the IHSBHN and IHSBM distributions provided competitive and often superior fits when compared with commonly used lifetime models.

From an engineering perspective, the flexibility of the proposed models in capturing diverse hazard rate behaviors makes them particularly suitable for modeling reliability data exhibiting non-standard failure patterns. This includes applications such as fatigue life analysis, degradation processes, and mechanical strength measurements, where traditional models may fail to adequately represent complex distributional features.

A natural direction for future research concerns the extension of the proposed IHSBHN and IHSBM distributions to regression settings. Since both models belong to a shape–scale family, with a positive scale parameter β, an accelerated failure time (AFT)–type formulation arises naturally by allowing the scale to depend on covariates.

Specifically, let $Y_i > 0$ denote a response variable and $\mathbf{z}_i$ a vector of covariates. An AFT-type IHSB regression model can be defined as $Y_i \mid \mathbf{z}_i \sim \text{IHSB}(\alpha, \beta_i)$, $\log(\beta_i) = \mathbf{z}_i^\top \gamma$, where γ is a vector of regression coefficients and α is a common shape parameter. Equivalently, the model admits the accelerated representation $Y_i = \beta_i Y_0$, with $Y_0 \sim \text{IHSB}(\alpha, 1)$.

This formulation provides a flexible and interpretable framework for modeling the effect of covariates on positive responses through a multiplicative scale structure. It is particularly well suited for lifetime data, such as fatigue life, but it can also be applied to positive mechanical strength measurements, such as tensile strength, where covariates act by accelerating or decelerating the scale of the response distribution. The development of estimation procedures, inference tools, and diagnostic methods for such AFT-type IHSB regression models constitutes an important topic for future studies.

Additional directions for future research include the extension of the proposed models to censored data settings, which are common in reliability and survival analysis, as well as the development of Bayesian estimation procedures that could provide further flexibility in inference and uncertainty quantification.

Author contributions

Ahmed M. Gemeay: contributed to the conceptualization, methodology, formal analysis, validation, investigation, and writing–review & editing; Yuri A. Iriarte: contributed to the conceptualization, software, formal analysis, validation, and writing–review & editing; Ohud A. Alqasem: contributed to the software, formal analysis, visualization, validation, and writing–original draft preparation; Fatma Masoud A. Zaghdoun: contributed to the software, formal analysis, visualization, validation, and writing–original draft preparation; Manahil SidAhmed Mustafa:

contributed to the methodology, formal analysis, visualization, validation, and investigation. All authors confirm that they have read and approved the published version of the manuscript.

Use of Generative-AI tools declaration

The authors declare they have not used Artificial Intelligence (AI) tools in the creation of this article.

Acknowledgments

Princess Nourah bint Abdulrahman University Researchers Supporting Project number (PNURSP2026R734), Princess Nourah bint Abdulrahman University, Riyadh, Saudi Arabia.

Conflict of interest

The authors declare no conflicts of interest.

References

1. R. A. Fisher, The effect of methods of ascertainment upon the estimation of frequencies, *Ann. Eugenics*, **6** (1934), 13–25.
2. C. R. Rao, On discrete distributions arising out of methods of ascertainment, *Sankhyā Indian J. Stat. Ser. A*, **27** (1965), 311–324.
3. M. Zelen, M. Feinleib, On the theory of screening for chronic diseases, *Biometrika*, **56** (1969), 601–614. https://doi.org/10.2307/2334668
4. G. P. Patil, J. Ord, On size-biased sampling and related form-invariant weighted distributions, *Sankhyā Indian J. Stat. Ser. B*, **38** (1976), 48–61.
5. G. P. Patil, C. R. Rao, The weighted distributions: a survey of their applications, *Appl. Stat.*, 1977, 383–405.
6. G. P. Patil, C. R. Rao, Weighted distributions and size-biased sampling with applications to wildlife populations and human families, *Biometrics*, 1978, 179–189.
7. R. C. Gupta, J. P. Keating, Relations for reliability measures under length biased sampling, *Scand. J. Stat.*, **13** (1986), 49–56.
8. B. O. Oluyede, On inequalities and selection of experiments for length biased distributions, *Probab. Eng. Inf. Sci.*, **13** (1999), 169–185.
9. K. K. Das, T. D. Roy, On some length-biased weighted weibull distribution, *Adv. Appl. Sci. Res.*, **2** (2011), 465–475.
10. G. Tzavelas, D. Panagiotakos, Statistical inference for the size-biased weibull distribution, *J. Stat. Comput. Simul.*, **83** (2013), 1252–1265. https://doi.org/10.1080/00949655.2012.657197
11. R. D. Gupta, D. Kundu, A new class of weighted exponential distributions, *Statistics*, **43** (2009), 621–634. https://doi.org/10.1080/02331880802605346

12. B. C. Arnold, R. J. Beaver, Hidden truncation models, *Sankhyā Indian J. Stat. Ser. A*, **62** (2000), 23–35.

13. A. Azzalini, A class of distributions which includes the normal ones, *Scand. J. Stat.*, **12** (1985), 171–178.

14. H. J. Kim, On a class of two-piece skew-normal distributions, *Statistics*, **39** (2005), 537–553.

15. B. C. Arnold, H. W. Gómez, H. S. Salinas, On multiple constraint skewed models, *Statistics*, **43** (2009), 279–293. https://doi.org/10.1080/02331880802357914

16. D. Elal-Olivero, Alpha-skew-normal distribution, *Proyecciones (Antofagasta)*, **29** (2010), 224–240. https://doi.org/10.4067/S0716-09172010000300006

17. H. Bolfarine, H. S. Salinas, H. W. Gómez, J. Arrué, A new class of skew-normal-Cauchy distribution, *Stat. Oper. Res. Trans.*, **39** (2015), 35–50.

18. N. L. Johnson, S. Kotz, N. Balakrishnan, *Continuous univariate distributions*, John Wiley & Sons, 2 Eds., 1994.

19. V. G. Vodă, Inferential procedures on a generalized rayleigh variate. I, *Appl. Math.*, **21** (1976), 395–412. https://doi.org/10.21136/am.1976.103663

20. N. L. Johnson, S. Kotz, N. Balakrishnan, *Continuous univariate distributions*, John wiley & Sons, 1995.

21. K. Soetaert, P. M. J. Herman, *A practical guide to ecological modelling: using R as a simulation platform*, Springer, 2009. https://doi.org/10.1007/978-1-4020-8624-3

22. K. Soetaert, *rootsolve: nonlinear root finding, equilibrium and steady-state analysis of ordinary differential equations*, R package version 1.6, 2009. Available from: `https://CRAN.R-project.org/package=rootSolve`.

23. R. H. Byrd, P. Lu, J. Nocedal, C. Zhu, A limited memory algorithm for bound constrained optimization, *SIAM J. Sci. Comput.*, **16** (1995), 1190–1208. https://doi.org/10.1137/0916069

24. W. Weibull, A statistical distribution function of wide applicability, *J. Appl. Mech.*, **18** (1951), 293–297. https://doi.org/10.1115/1.4010337

25. R. D. Gupta, D. Kundu, Theory & methods: generalized exponential distributions, *Aust. N. Z. J. Stat.*, **41** (1999), 173–188. https://doi.org/10.1111/1467-842X.00072

26. J. Faraway, G. Marsaglia, J. Marsaglia, A. Baddeley, *Goftest: classical goodness-of-fit tests for univariate distributions*, R package version 1.2-3, 2021. Available from: `https://CRAN.R-project.org/package=goftest`.

27. H. Akaike, A new look at the statistical model identification, *IEEE Trans. Autom. Control*, **19** (1974), 716–723. https://doi.org/10.1109/TAC.1974.1100705

28. G. Schwarz, Estimating the dimension of a model, *Ann. Stat.*, **6** (1978), 461–464. https://doi.org/10.1214/aos/1176344136

29. R. Shanker, K. Shukla, On modeling of lifetime data using three-parameter generalized lindley and generalized gamma distributions, *Biom. Biostat. Int. J.*, **4** (2016), 283–288. https://doi.org/10.15406/bbij.2016.04.00117

30. M. Bader, A. Priest, Statistical aspects of fibre and bundle strength in hybrid composites, *Progress Sci. Eng. Compos.*, 1982, 1129–1136.

31. G. Grimmett, D. Stirzaker, *Probability and random processes*, Oxford University Press, 2020.

Appendix

Appendix A. Moments for a positive random variable

Lemma 1. *Let $X \geq 0$ be a nonnegative random variable with distribution function*

$$F(x) = \mathbb{P}(X \leq x)$$

and survival function

$$S(x) = 1 - F(x) = \mathbb{P}(X > x).$$

If $\mathbb{E}[X^r] < \infty$ for some $r \geq 1$, then

$$\mathbb{E}[X^r] = \int_0^\infty r\, x^{r-1}\, S(x)\, dx.$$

Proof. Starting from the general definition of the rth moment,

$$\mathbb{E}[X^r] = \int_0^\infty x^r\, dF(x).$$

Since

$$x^r = \int_0^x r\, t^{r-1} dt,$$

it follows that

$$\mathbb{E}[X^r] = \int_0^\infty \left(\int_0^x r\, t^{r-1}\, dt \right) dF(x).$$

By the Fubini–Tonelli theorem, which allows the interchange of the order of integration for nonnegative functions, it follows that

$$\mathbb{E}[X^r] = \int_0^\infty r\, t^{r-1} \left(\int_t^\infty dF(x) \right) dt.$$

Noting that

$$\int_t^\infty dF(x) = 1 - F(t) = S(t),$$

we obtain

$$\mathbb{E}[X^r] = r \int_0^\infty t^{r-1} S(t)\, dt.$$

This completes the proof. □

Adapted from [31].

Appendix B. Summary of the IHSB framework and its induced distributions

Table 10. Structure of the IHSB construction for different baseline distributions and resulting models.

Baseline model	Baseline PDF	Baseline parameter	Role of α	Resulting model
Exponential	$\frac{1}{\beta}e^{-x/\beta}$	$\beta > 0$ (scale)	$\alpha > 0$ (shape)	Gamma
Rayleigh	$2\theta x e^{-\theta x^2}$	$\theta > 0$ (scale)	$\alpha > 0$ (shape)	Generalized Rayleigh
Lomax (Pareto II)	$\gamma(1+x)^{-(\gamma+1)}$	$\gamma > 0$ (shape)	$0 < \alpha < \gamma$	Beta prime
Half-normal	$\frac{2}{\beta}\phi(x/\beta)$	$\beta > 0$ (scale)	$\alpha > 0$ (shape)	IHSBHN (new)
Maxwell	$\frac{2}{\sqrt{\pi}}\frac{x^2}{\beta^3}e^{-x^2/(2\beta^2)}$	$\beta > 0$ (scale)	$\alpha > 0$ (shape)	IHSBM (new)

Note: The parameter α induces additional flexibility in the shape of the resulting density function relative to the baseline distribution. In particular, it allows for a wider range of skewness and kurtosis values, encompassing those of the baseline model as special cases.

AIMS Press